

Electronic Supporting Information (ESI†)

for

Synthesis, characterization, and cancer cell-selective cytotoxicity of mixed-ligand cobalt(III) complexes of 8-hydroxyquinolines and phenanthroline bases

Banashree Deka,^{a‡} Tukki Sarkar,^{a‡,§} Arnab Bhattacharyya,^b Ray J. Butcher,^{*c} Samya Banerjee,^{*d} Sasanka Deka,^e Kandarpa K. Saikia^{*f} and Akhtar Hussain^{*a}

^a Department of Chemistry, Handique Girls' College, Guwahati 781001, Assam, India. E-mail: akhtariisc@gmail.com

^b Department of Inorganic and Physical Chemistry, Indian Institute of Science, Bangalore 560 012, Karnataka, India.

^c Department of Chemistry, Howard University, 525 College Street NW 20059, USA. E-mail: rbutcher99@yahoo.com

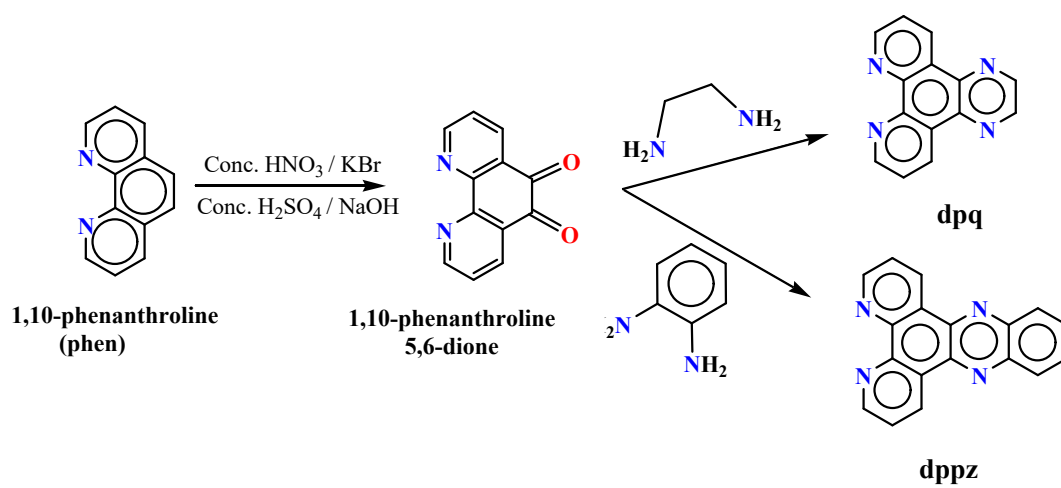
^d Department of Chemistry, Indian Institute of Technology (BHU), Varanasi, UP 221005, India. E-mail: samya.chy@itbhu.ac.in

^e Department of Chemistry, University of Delhi, New Delhi 110024, India. E-mail: ssdeka@gmail.com

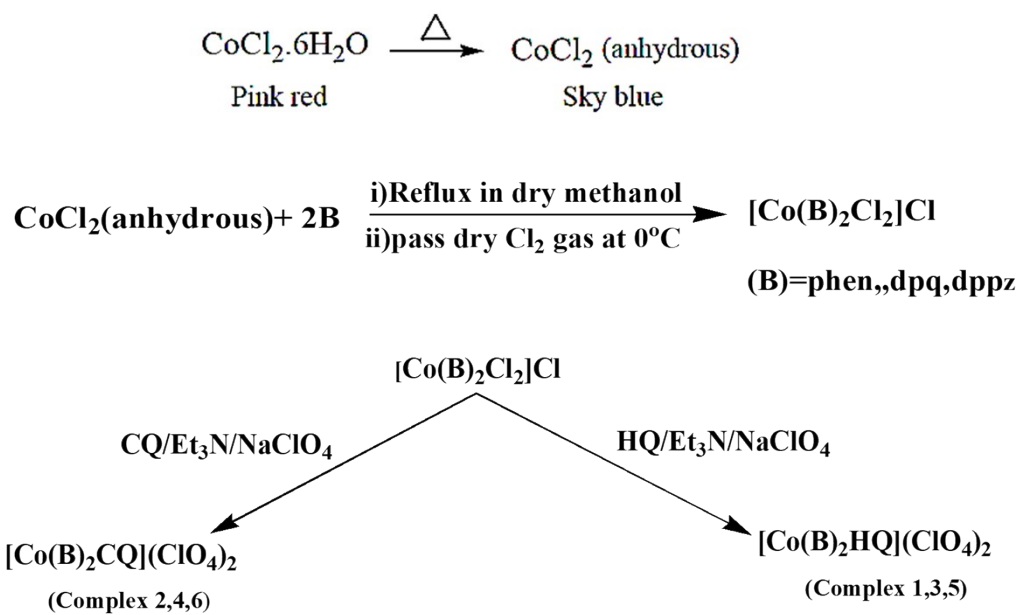
^f Department of Bioengineering and Technology, GUIST, Gauhati University, Guwahati 781014, Assam, India. E-mail: kksaikia@gmail.com

[‡] These authors contributed equally to the work.

[§] Present address; Department of Fluoro-Agrochemicals, CSIR-Indian Institute of Chemical Technology, Hyderabad 500007, Telangana, India.



Scheme S1. Schematic representation showing the synthetic route to dpq and dppz ligands.



Scheme S2. A generalized reaction scheme showing the synthesis of complexes 1–6.

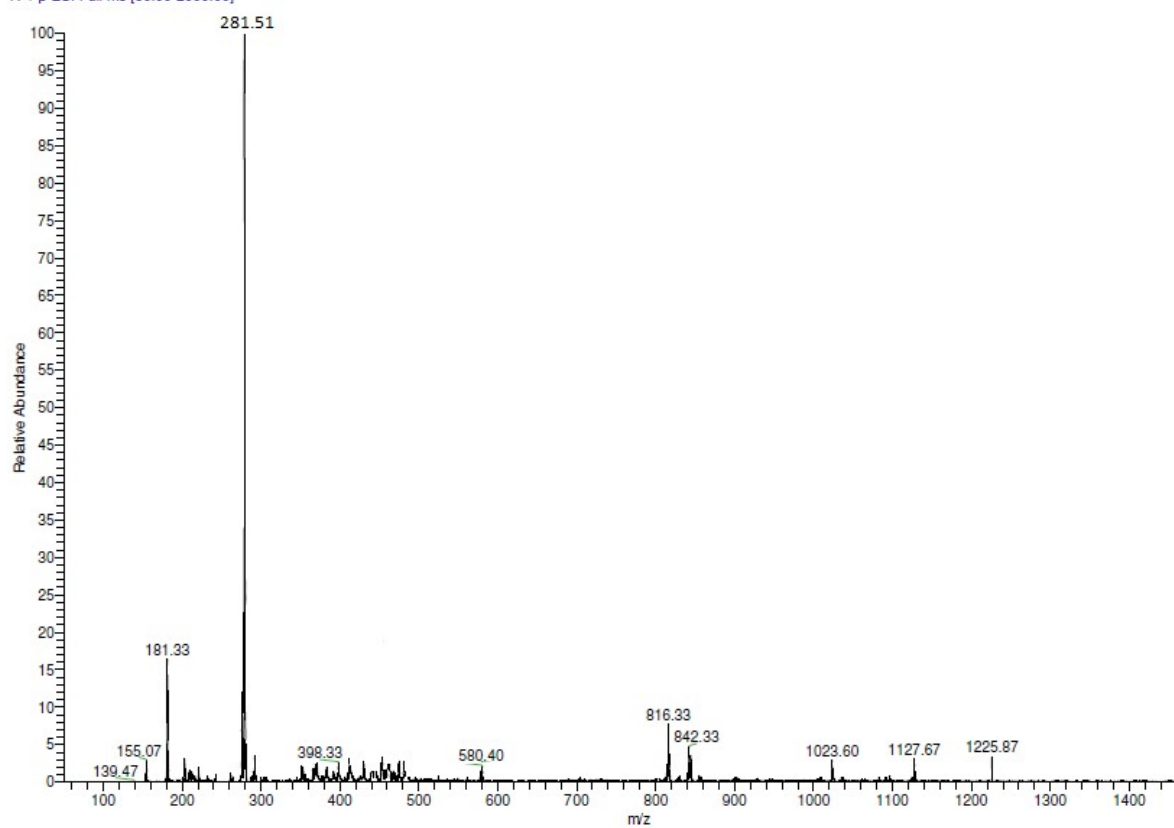


Fig. S1. The ESI-MS spectrum of $[\text{Co}(\text{phen})_2(\text{HQ})](\text{ClO}_4)_2$ (**1**) in 10% aqueous MeOH/MeCN (1:1 ratio) showing the $[\text{M}-2(\text{ClO}_4^-)]^{2+}$ peak.

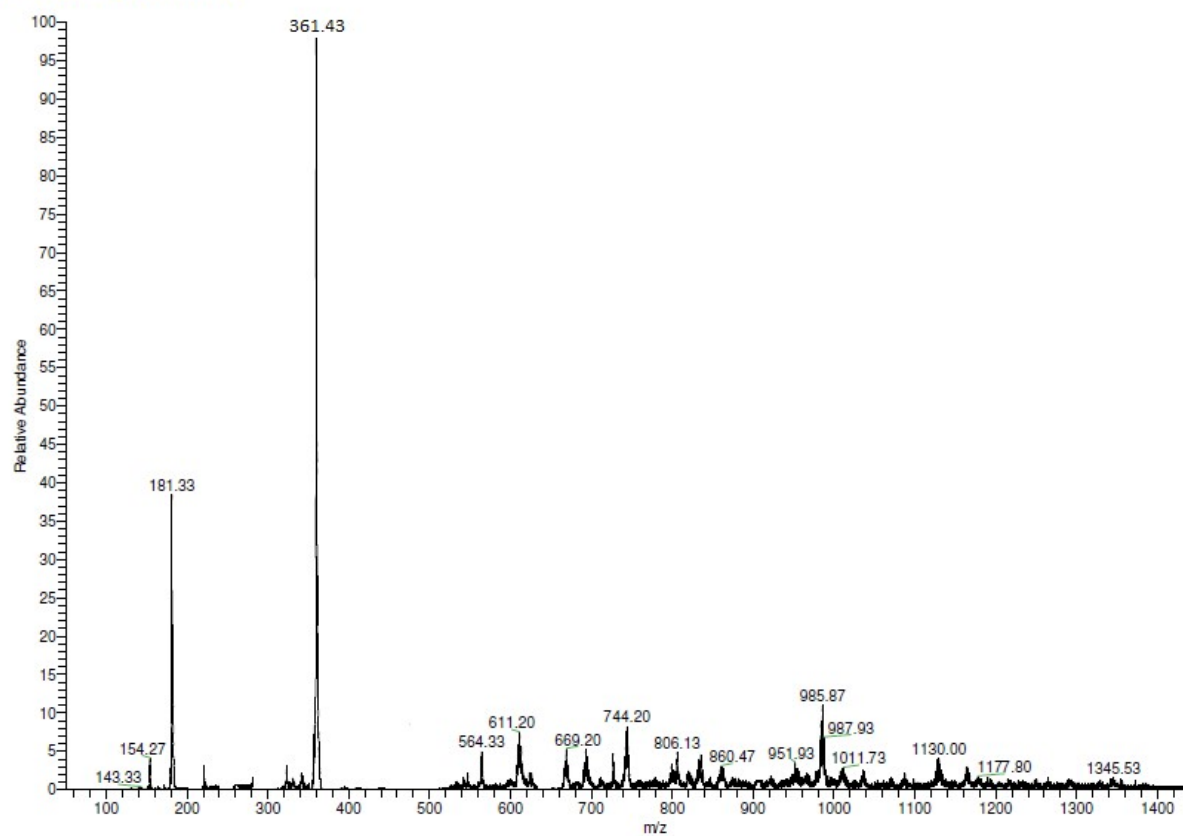


Fig. S2. The ESI-MS spectrum of $[\text{Co}(\text{phen})_2(\text{CQ})](\text{ClO}_4)_2$ (**2**) in 10% aqueous MeOH/MeCN (1:1 ratio) showing the $[\text{M}-2(\text{ClO}_4^-)]^{2+}$ peak.

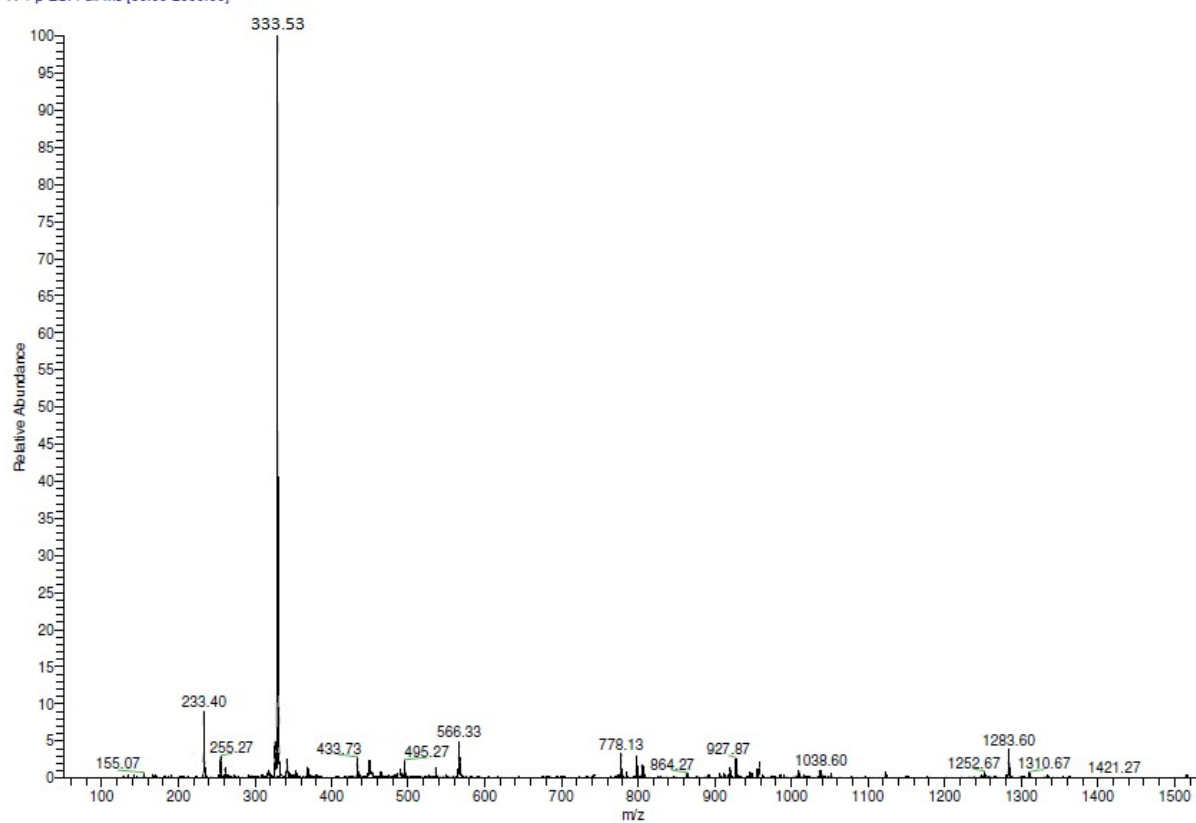


Fig. S3. The ESI-MS spectrum of $[\text{Co}(\text{dpq})_2(\text{HQ})](\text{ClO}_4)_2$ (**3**) in 10% aqueous MeOH/MeCN (1:1 ratio) showing the $[\text{M}-2(\text{ClO}_4^-)]^{2+}$ peak.

Diluted in MeOH
T: + p ESI Full ms [50.00-2000.00]

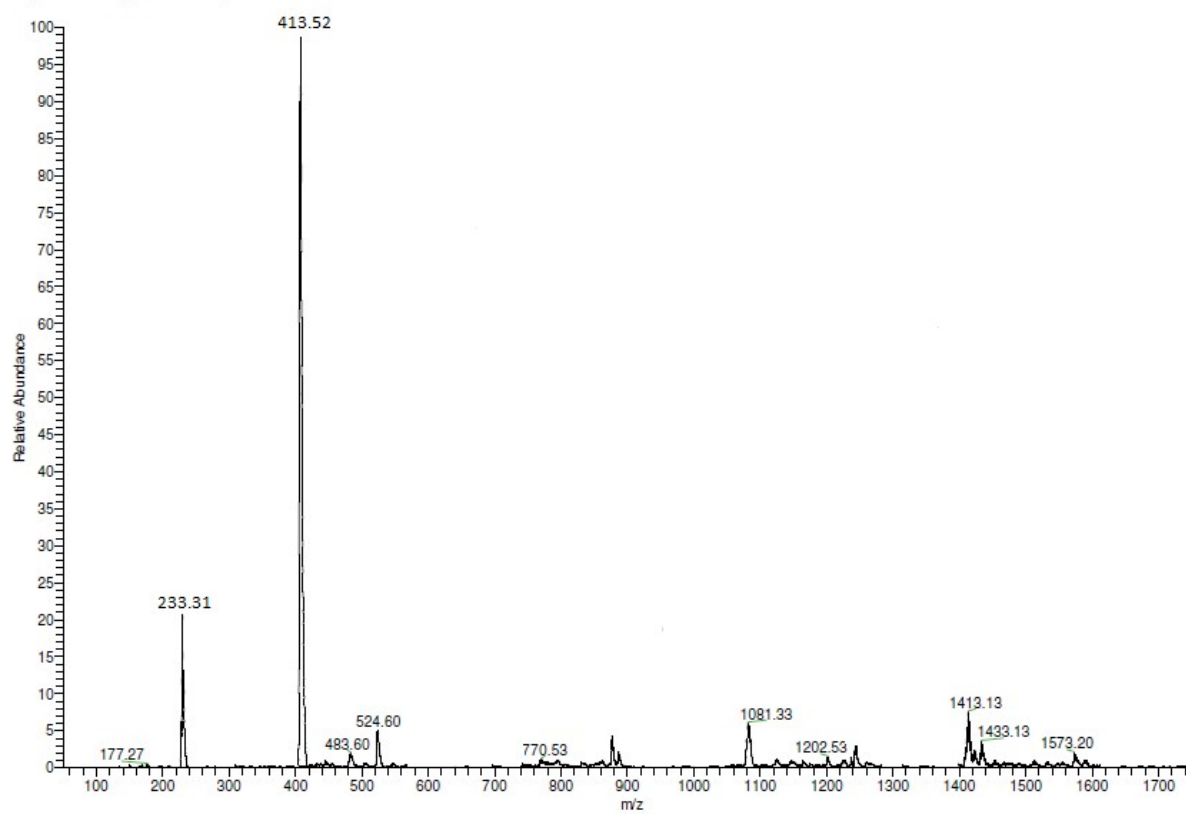


Fig. S4. The ESI-MS spectrum of $[\text{Co}(\text{dpq})_2(\text{CQ})](\text{ClO}_4)_2$ (**4**) in 10% aqueous methanol showing the $[\text{M}-2(\text{ClO}_4^-)]^{2+}$ peak.

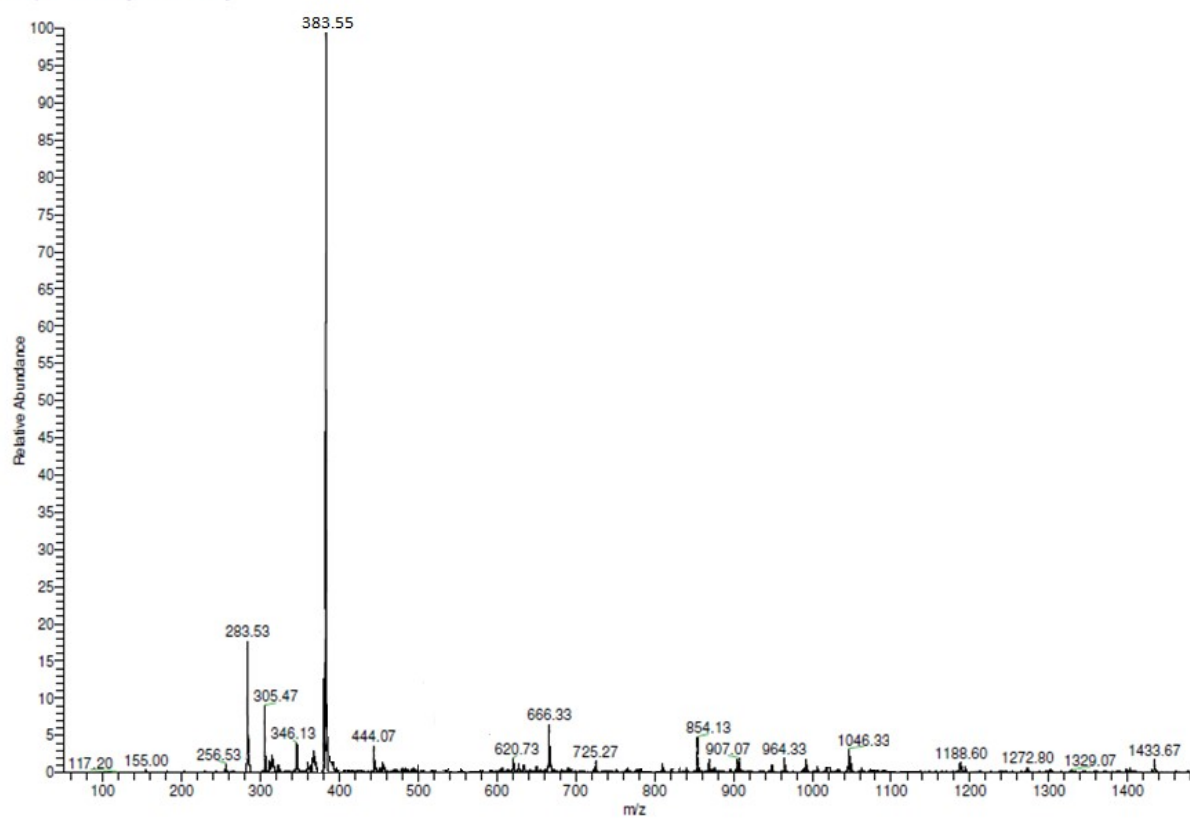


Fig. S5. The ESI-MS spectrum of $[\text{Co}(\text{dppz})_2(\text{HQ})](\text{ClO}_4)_2$ (**5**) in 10% aqueous MeOH/MeCN (1:1 ratio) showing the $[\text{M}-2(\text{ClO}_4^-)]^{2+}$ peak.

Diluted in ACN

T: + p ESI Full ms [50.00-2000.00]

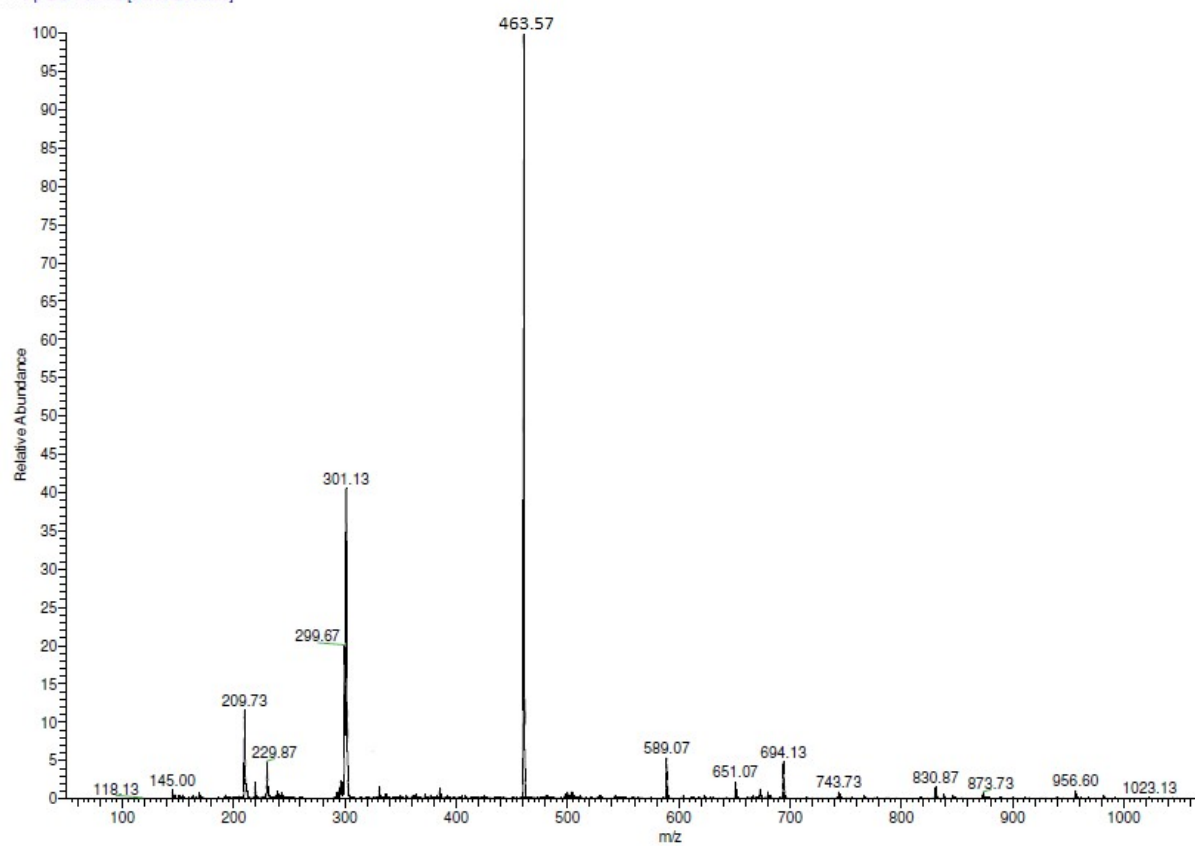


Fig. S6. The ESI-MS spectrum of $[\text{Co}(\text{dppz})_2(\text{CQ})](\text{ClO}_4)_2$ (**6**) in 10% aqueous MeCN showing the $[\text{M}-2(\text{ClO}_4^-)]^{2+}$ peak.

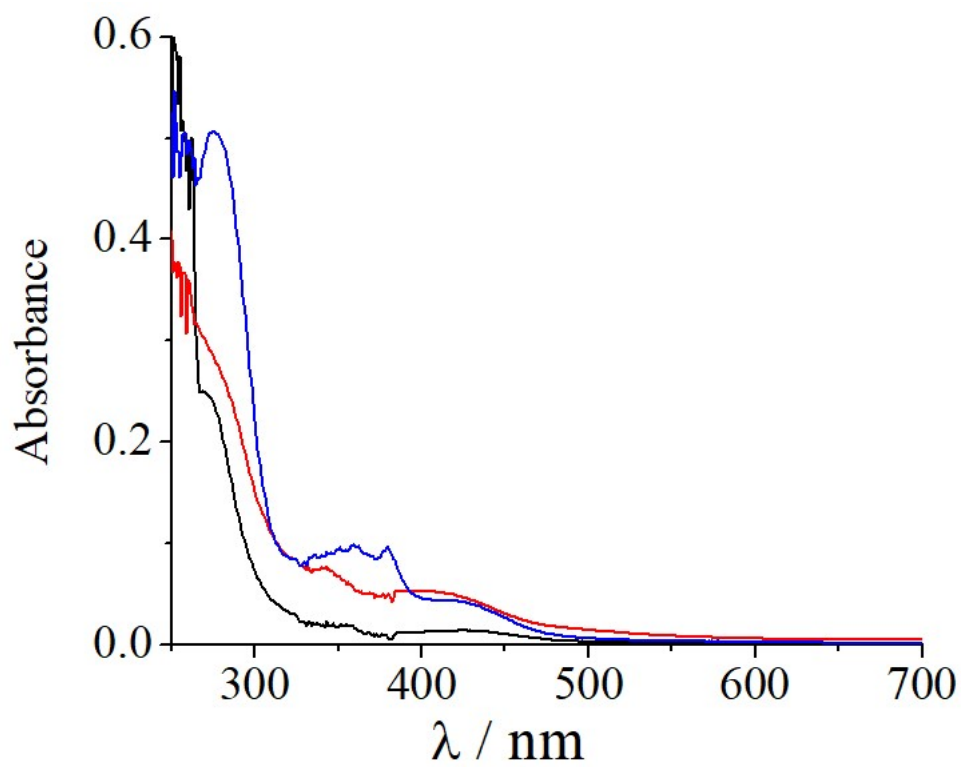


Fig. S7. The electronic absorption spectra of complexes **1** (black), **3** (red), and **5** (blue) in DMF/PBS [1:9 (v/v), pH = 7.2).

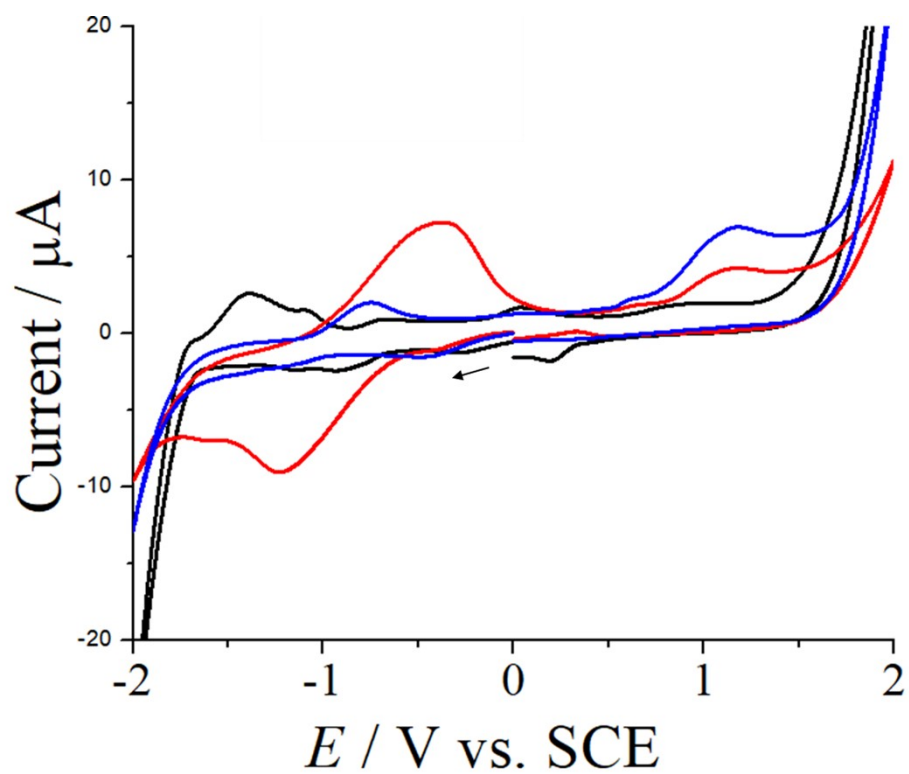


Fig. S8. The cyclic voltammograms of complexes **1** (blue), **3** (red), and **5** (black) measured in 5:1 (v/v) DMF/PBS (0.1 M TBAP) showing the cathodic and anodic peaks.

Table S1. Cyclic voltametric data for complexes **1–6** (V. vs. SCE, 0.1 M TBAP) showing the cathodic and anodic peaks.

Complex	E_{pc1}	E_{pc2}	E_{pc3}	E_{pa1}	E_{pa2}	E_{pa3}	E_{pa4}
1	-0.44	-	-		1.16	-	-
2	-0.93	-	-	-0.72	-1.40	-	-
3	-1.22	-	-	-	-0.35	1.17	-
4	-1.57	-0.83	-0.26	-1.46	-0.72	-	0.35
5	-0.90	-0.20	0.20	-0.70	0.30	-	-1.40
6	-0.93	-0.24	-	-0.70	-	-1.45	0.32

Note: E_{pc1} and E_{pa2} , E_{pc2} and E_{pa2} , E_{pc3} and E_{pa3} are the corresponding counterparts of cathodic and anodic peaks. Cathodic and anodic peaks with no counterparts are written in separate columns in the table.

Table S2. Selected crystallographic data and structure refinement parameters for the complexes **1a** and **2a**.acetone.

Empirical formula	C ₃₃ H ₂₂ N ₅ OF ₁₂ P ₂ Co	C ₃₃ H ₂₅ N ₅ OF ₁₂ P ₂ ClCo
	(1a)	(2a .acetone)
Formula weight (gmol ⁻¹)	853.42	1018.80
Crystal system	Monoclinic	Monoclinic
Space group	<i>P21/n</i>	<i>P21/c</i>
<i>a</i> (Å)	10.542(2)	13.3417(5)
<i>b</i> (Å)	18.441(4)	17.9204(7)
<i>c</i> (Å)	19.009(4)	16.6565(6)
α (°)	90.000	90.000
β (°)	90.05(3)	92.157(2)
γ (°)	90.000	90.000
<i>V</i> (Å ³)	3695.6(13)	3979.6(3)
<i>Z</i>	4	4
<i>T</i> (K)	296(2)	296(2)
ρ_{calc} (g cm ⁻³)	1.534	1.700
λ Å (Mo- <i>K</i> α)	0.71073	0.71073
μ (mm ⁻¹)	0.646	1.446
Data/restraints/parameters	10800/132/526	11602/0/541
<i>F</i> (000)	1712	2004
Goodness-of-fit on <i>F</i> ²	1.057	1.020
<i>R</i> (<i>F</i> _o) ^a , I>2 σ (I) / <i>wR</i> (<i>F</i> _o) ^b	0.0732/0.2085	0.0747/0.2079
<i>R</i> (all data)/ <i>wR</i> (all data)	0.1668/0.2576	0.1654/0.2610
Largest diff. peak and hole (e Å ⁻³)	0.663, -0.395	-1.036, -1.036

^a*R* = $\Sigma||F_o|-|F_c||/\Sigma|F_o|$. ^b*wR* = $\{\Sigma[w(F_o^2-F_c^2)^2]/\Sigma[w(F_o^2)]\}^{1/2}$; $w = [\sigma^2(F_o)^2 + (AP)^2 + BP]^{-1}$, where $P = (F_o^2 + 2F_c^2)/3$, A = 0.1307, B = 1.1418 for complex **1a**; A = 0.1345, B = 0.0000 for complex **2a**. acetone.

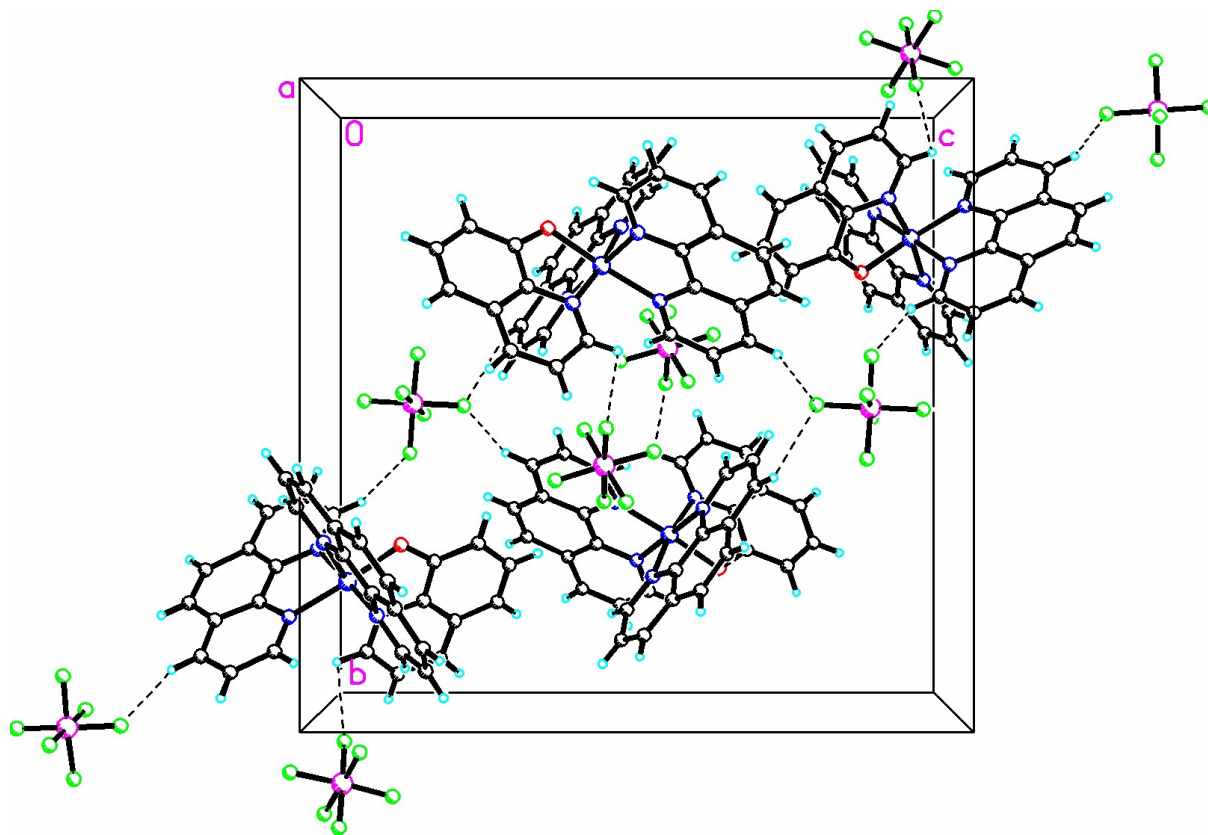


Fig. S9. The unit cell packing diagram of $[\text{Co}(\text{phen})_2(\text{HQ})](\text{PF}_6)_2$ (**1a**). The complex crystallized in the $P2_1/n$ space group with $Z = 2$.

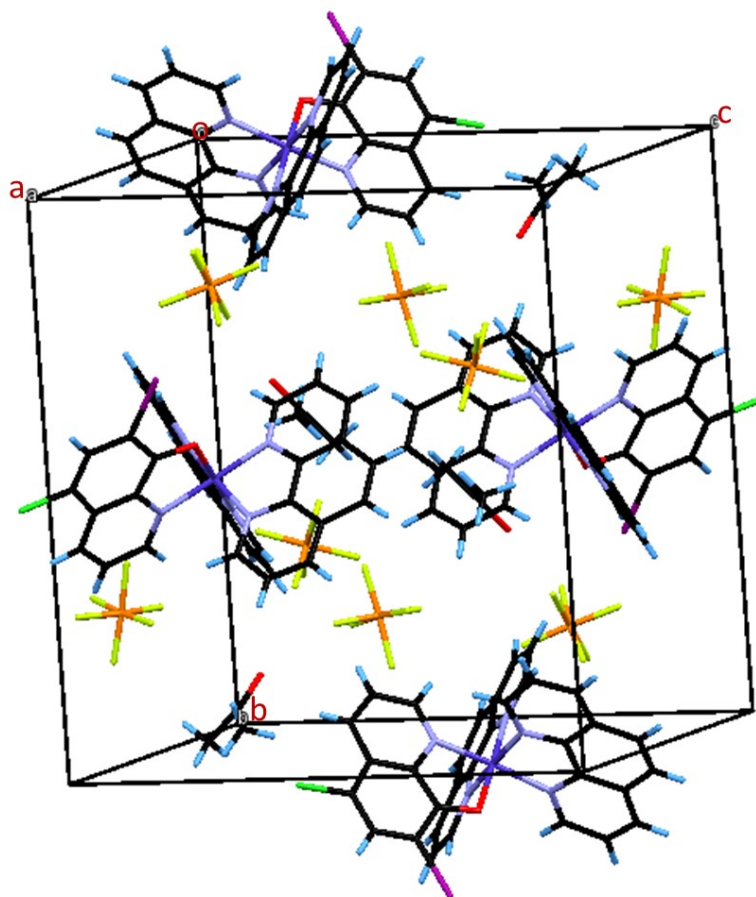


Fig. S10. The unit cell packing diagram of $[\text{Co}(\text{phen})_2(\text{CQ})](\text{PF}_6)_2 \cdot \text{acetone}$ (**2a.acetone**). The complex crystallized in the monoclinic $P2_1/c$ space group with $Z = 4$.

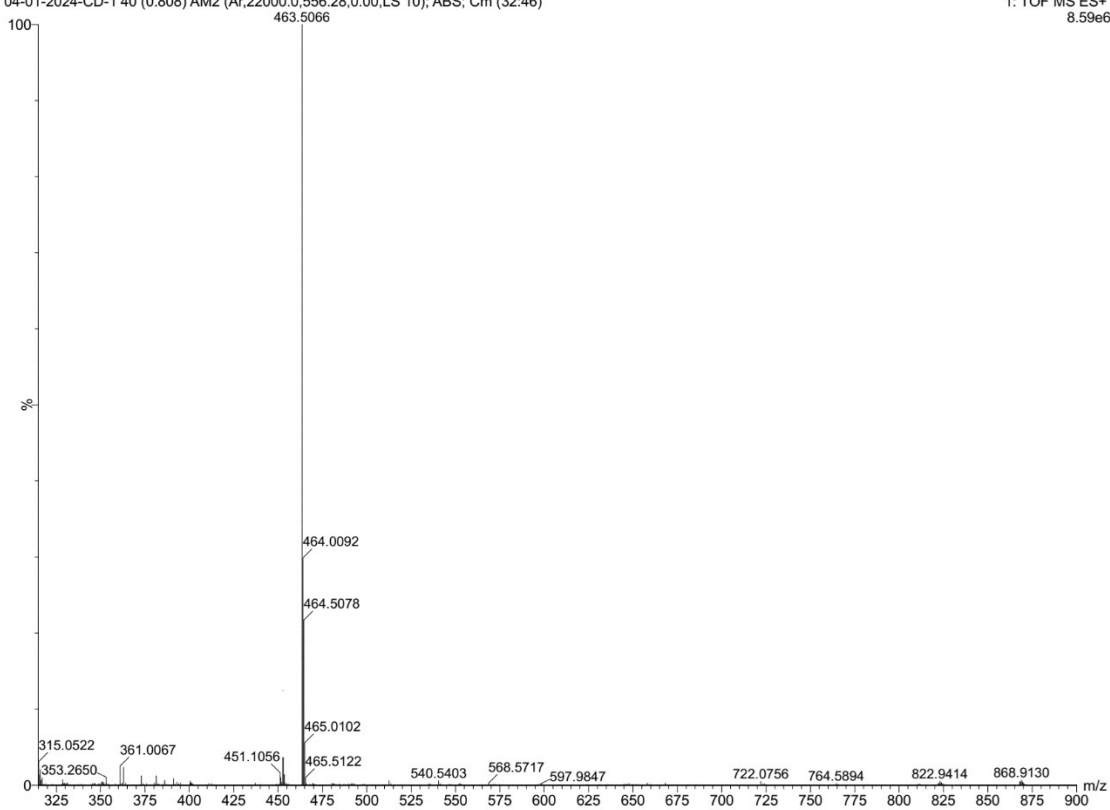


Fig. S11. HRMS (TOF MS ES+) spectrum of complex **6** using 10% (v/v) aqueous acetonitrile after 48 hours. The complex retained the molecular ion peak corresponding $[M-2(\text{ClO}_4)]^{2+}$ at m/z 463.5066.

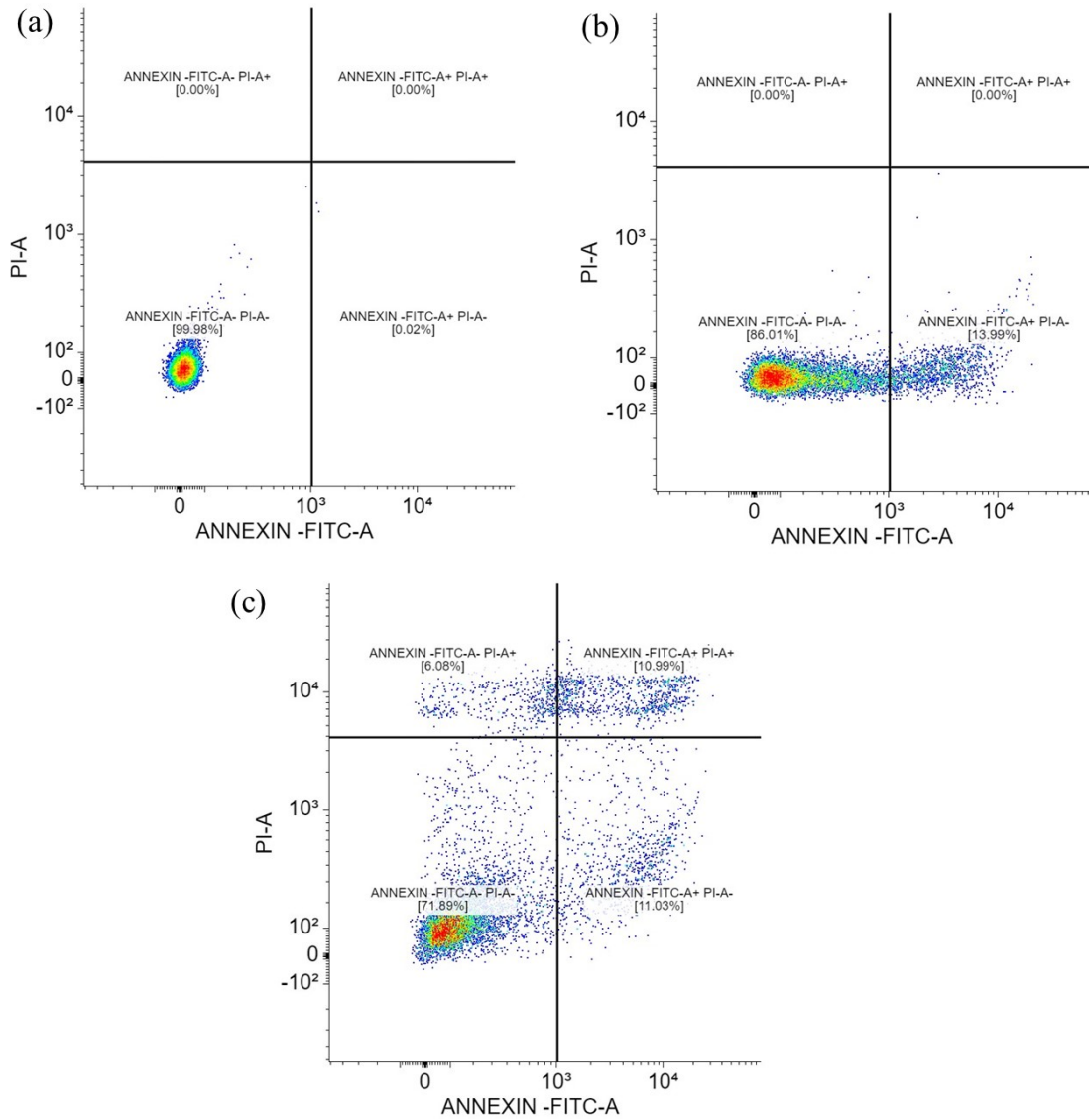


Fig. S12. Annexin V-FITC/PI coupled flow cytometric analysis showing various controls with HeLa cells: (a) Cells only; (b) Cells + Annexin-V-FITC only; (c) Cells + Annexin-V-FITC + PI.